Optimization of Fuel Assembly Allocation
for Boiling Water Reactors

Hiroshi MOTODA and Osamu YOKOMIZO

*Atomic Energy Research Laboratory, Hitachi Ltd.**

A direct search algorithm is applied to the optimization of fuel assembly allocation of BWR with particular consideration given to the nuclear model and the treatment of operating constraints. A simple expression is derived for evaluating the stuck rod margin, based on regression analysis of data obtained by three-dimensional full core analysis, and the expression is applied to optimization procedure.

The practical applicability of the method is confirmed through trial computations for the second and equilibrium cycles of a medium-sized commercial BWR, with an examination based on various initial guesses and objective functions for radial power peaking.

KEYWORDS: *optimization, direct search, fuel loading, refueling schedule, BWR type reactors, stuck rod margin, simulation, power distribution, power peaking, control rods, fuel asssembly*

I. INTRODUCTION

Optimization of in-core fuel management is of great importance on account of its effect on nuclear reactor economy. Complete optimization to cover the entire reactor lifetime, however, is very difficult because of the large number of decision variables to be dealt with and the complexity of the system. In whatever manner the problem is formulated, it inevitably becomes a large scale optimization problem if the results are to be of any practical value.

It is thus natural that past studies have mostly adopted an extremely simplified model for solving long term optimization problems, and have laid aside the question of detailed fuel assembly allocation[1]~[4]. More recent studies on individual fuel assembly allocation, on the other hand, have limited their scope to short range problems[5][6] or else to an equilibrium cycle analysis[7] with effort concentrated on devising the reactor model to be adopted.

It is definitely desirable from the viewpoint of core management of an actual operating reactor to establish a realistic core model that will permit optimal or at least sub-optimal determination of the individual fuel assembly allocations in initial and replacement core loadings, and yield a realistic design and operating constraints, without demanding excessive computing time. Naft & Sesonske[5] have developed a direct search algorithm for optimizing the fuel shuffling pattern such that radial power peaking was minimized. A similar problem was studied by Stout & Robinson[6] using an automated search procedure based on predetermined shuffling rules. This was followed by Chitkara & Weisman[7] who optimized the refueling procedure and core power at equilibrium by means of an assignment and direct search algorithm. Kubokawa & Kiyose[8] utilized linear integer programming for optimizing the fuel loading procedure and control rod programming.

A logical approach to this large scale optimization problem would be the adoption of a hierarchical method, *i.e.* separation of the total problem into coupled sub-problems[9]~[15]. Optimization of each sub-problem is performed first, followed by coordination of the solutions

to the sub-problems to obtain an overall optimal (or failing this a locally optimum) solution. Studies on the determination of detailed fuel loading patterns can be considered a sub-problem in the overall system.

OPREF is a computer program[16] developed in an effort to satisfy the above requirement by a top-downward hierarchical approach. One of its characteristics is that it has an automated optimization package for fuel assembly allocation. It seeks a fuel assembly loading pattern such that radial power peaking is minimized with use made of the direct search algorithm proposed by Naft & Sesonske[5].

The objective of the present paper is to consider this package in more detail, particularly in regard to the explicit inclusion of a stuck rod margin constraint which is one of the most important design and operating criteria for the BWR (Boiling Water Reactor), and which was taken into account only in a global form in the first version of OPREF. The practical applicability of the method is confirmed by trial computations for the optimization of the second and equilibrium cycle core loading patterns of a commercial BWR of 460 MWe.

II. OPTIMIZATION PROCEDURE

1. Definition of Problem

The problem is to allocate the fuel assemblies in a core such that the radial power peaking is minimized. Power distribution inherently changes with burnup, whose process is determined by control rod programming. The degree of freedom of power distribution control decreases towards the EOC (end of cycle), at which stage there are practically no rods remaining inserted in the core.

The optimization procedure must be performed in respect of this estimated EOC state, with consideration given separately to the effects of control rod programming and of loading pattern optimization. Haling operation[17] was assumed in calculating the EOC exposure distribution. Once the fuel loading pattern has been optimized, the actual operating strategy can be determined by a three-dimensional control rod programming gener-

ator OPROD[18], such as to minimize the deviation at EOC of the calculated exposure distribution from the target configuration.

The constraints to be considered here are: (1) Immobilized fuel assemblies, if any and (2) stuck rod margin. The first constraint is mainly used to fix the locations of some of the assemblies and prevent these assemblies, once fixed, from being moved to other locations. This constraint could possibly be utilized for dealing with failed fuel assemblies, by transferring them to a region of lower power density for immobilization until such time as they could be discharged. (Note: Rules now in force do not permit failed assemblies to remain in the core.)

The second constraint provides for an accident involving the sticking of a single control rod. When any one rod is prevented for any reason from being inserted normally, the reactor should still possesses a minimum margin of subcriticality at cold state by the remaining rods. All eligible fuel loading patterns must necessarily satisfy this condition for the sticking of any control rod at all stages of fuel burnup.

It is assumed that the number and choice of assemblies to be discharged at each step is predetermined at the time of optimization. This is considered to be determined by a regionwise shuffling scheme optimized as the solution of a sub-problem of higher ranking in OPREF. In other words, no assembly shuffling between different regions is performed unless there is reason to consider it definitely necessary.

2. Direct Search Algorithm

The allocation of individual fuel assemblies is optimized by means of a direct search algorithm, originally proposed by Naft & Sesonske[5], and slightly modified.

The possible combination of allocation patterns is $\prod_{k=1}^{N_{reg}} N_{asse_k}!$, where N_{reg} represents the number of regions, and N_{asse_k} the number of assemblies in region k. This amounts to as much as 1.216×10^{19} for only the quarter-core analysis of a medium sized BWR comprising five regions, each of 20 assemblies ($5 \times 20!$).

Direct enumeration of all the possible patterns would require about 4×10^{12} yr in computing time, assuming 10 sec to calculate the Haling power distribution of one refueling pattern. Some drastic simplification is thus called for.

The method adopted in the present instance is a kind of univariable approach. The number of combinations of possible dual exchanges of fuel assemblies is thereby reduced to $\prod_{k=1}^{N_{reg}} N_{asse_k} C_2$, which corresponds to a value of only 950 for the same reactor as above. In view of this commensurate reduction obtained on the number of combinations, the following direct search algorithm is proposed as a practical method of optimization.

The optimization scheme is in three modes: exploratory, standard, and exhaustive search. In the exploratory search mode, each variable is exchanged with every other variable. For each exchange, the objective function is the maximum value of power which is defined in the next section. A table is generated covering N_{table_k} (input specified) best choices for the first N_{try_k} (input specified) ranked assemblies in the selected region k. Noted in these tables numbering N_{pord} (input specified) are the power peaking values, the assembly numbers and the number of the assembly with which each assembly is to be exchanged.

When the exploratory search mode is completed, the operation is advanced to the standard search mode. The N_{pord} tables of exchanges are searched for the assembly with the lowest value of the objective function. When this is found, a trial exchange is made. If the objective function is an improvement over the last guess, the exchange is finalized and all other shufflings in the table that include these assemblies are discarded, to form a new basis. A search is again made of the tables to determine the next best move. The new objective function is checked to determine if an improvement has been achieved. If so found, all table entries containing the relevant assemblies are discarded, to constitute a further new basis. If not, the assemblies relevant to this exchange are discarded from the table and the next lowest value in these tables is sought, and the process is re-

peated. This pattern of search continues until all entries in these tables have been utilized or until N_{fail} (input specified) successive choices have ended in failure. When either case occurs, the exploratory search is again called and the entire process is repeated.

If the search pattern does not indicate convergence toward an optimum, the exhaustive search mode is called. In this case only one base point move is made after every exploratory search.

The principle is to make the best use of each table, once it is created. The table is made to serve as guide for deciding the direction in which the assembly should be moved.

(1) Exploratory Search Mode

The generation of tables to cover all regions is unnecessary because fuel assemblies in the low power regions usually do not produce power peaking. Furthermore, it is not necessary to examine all the possible combinations of assembly exchanges in the region where the table is to be made because it rarely happens that replacing a high power assembly with one of low power will not reduce the power peaking.

Based on the above observations, we establish the following rules for generating the tables.

(i) Only regions where the maximum power densities are ranked within the first N_{pord} are considered for fuel shuffling. Fuel assemblies in other regions are immobilized. This criterion is applied every time a new table is generated. Thus, the regions considered for reshuffling will vary from time to time in the process of every exploratory search. Shuffling in all regions can be made by letting $N_{pord} = N_{reg}$.

(ii) In each region considered for reshuffling, the fuel assemblies are numbered sequentially from the maximum toward minimum power. Tables are generated to include only the assemblies ranked within the first N_{try_k}, for the purpose of finding the most eligible assemblies for exchange amounting in number to N_{table_k} (*i.e.* for a region k considered for reshuffling,

a table of the scope of $N_{\mathrm{try}_k} \times N_{\mathrm{table}_k}$ is generated).

(iii) Fuel assemblies whose infinite multiplication factors at EOC are within ε_1 are regarded as possessing the same nuclear properties. For such assemblies, the power distribution calculation for the trial exchange of assemblies is skipped, and the base point values are stored.

(iv) With a view to saving computer time, two modes are prepared—normal and rapid. These differ in the allowed maximum number of source and void loop iterations. Each time before the exploratory search mode is started, a Haling power distribution for a fixed cycle length is calculated by normal mode to determine the initial base point. No heed is taken of the differences in cycle length between the various patterns. It is taken for granted that shuffling within one region does not affect the cycle length.

The rapid mode is adopted for calculating the power distribution in exploratory search, since this is the most time consuming part of the whole optimization scheme.

(2) Standard Search Mode

When the lowest objective function value is sought, a trial exchange is made by rapid mode. If the resultant maximum power density P_{max} satisfies the relation $P_{\mathrm{max}} - P_{\mathrm{base}} < \varepsilon_2$, the trial is regarded as an intermediate success, where P_{base} stands for the maximum power of the latest base point. In such case, the power distribution is recalculated by the normal mode.

If this results in $P_{\mathrm{base}} \leqslant P_{\mathrm{max}}$, this trial is a failure and the shuffling scheme is discarded from the table. The search is resumed on the table to determine the next best move. If a success is obtained ($P_{\mathrm{base}} > P_{\mathrm{max}}$), this trial is terminated and the base point altered. All other shufflings in the table that include these assemblies are discarded from the table. If the success is in the first entry and $|P_{\mathrm{base}} - P_{\mathrm{max}}| \leqslant \varepsilon_2$, it is considered that there is no meaningful reduction of the power. If such a relation is satisfied N_{first} (input specified) times in succession, an optimum pattern is regarded to have been obtained.

If the rapid mode trial results in failure ($P_{\mathrm{max}} - P_{\mathrm{base}} \geqslant \varepsilon_2$), this shuffling is discarded from the table and a search is again made of the tables to determine the next best move. If the first entry is a failure, an optimal pattern is regarded to have been achieved.

Each time before starting a search in the exploratory mode, the initial base point value P_{base}^{Nt} is compared with the previous value P_{base}^{Nt-1}. If $P_{\mathrm{base}}^{Nt} - P_{\mathrm{base}}^{Nt-1} \geqslant \varepsilon_3$, an optimal pattern is again regarded to have been reached.

It is to be noted that when a trial ends in failure, only the table relevant to the region in question is discarded.

(3) Exhaustive Search Mode

If the exploratory search results in N_{exhas} (input specified) successive failures upon rapid mode trial in the second entry, the search is advanced to exhaustive mode. In this mode, the standard search is skipped and only the first entry is tried.

The optimization process described above is recapitulated in the form of a block diagram in **Fig. 1**.
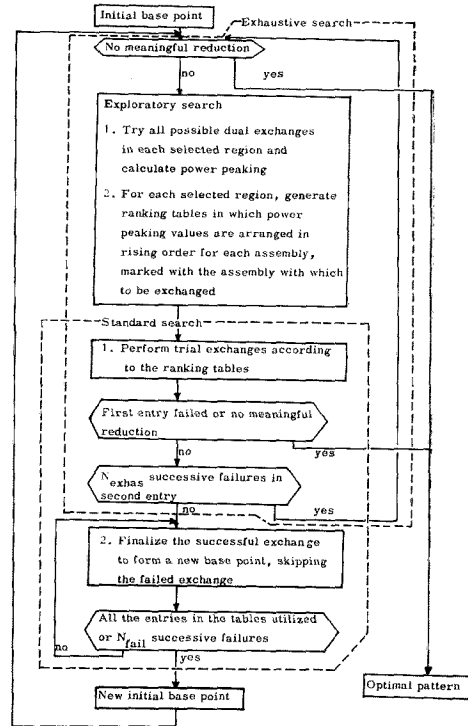

Fig. 1 Simplified block diagram of optimization process

3. Objective Function for Radial Power Peaking

The aim of optimization is to minimize the radial power peaking factor. Thus, the direct objective function is the maximum value of assembly power densities. The Haling distribution is adopted as power distribution in this paper. Since it is very time-consuming to calculate the Haling power distribution thousands of times even by means of the rapid mode, a number of alternative objective functions are proposed to serve as power peaking index:

Method A The Haling power distribution is calculated by the normal mode each time before initiation of the exploratory search mode, to serve as the initial base point. In this search mode, the normal power distribution is calculated by the rapid mode with k_∞ of the initial base point replaced. In the standard search mode normal power distribution is calculated first by the rapid mode, and if the trial is a success, the power distribution is recalculated by the normal mode.

Calculation of the normal power distribution does not require void loop iteration because the estimated EOC k_∞ distribution is taken from the initial base point. The normal power distribution, therefore, approximates the EOC power distribution which in turn is an approximation of the Haling distribution.

Method B The Haling power distribution is calculated for all occasions, with the rapid and normal modes used in the same nammer as in Method A. This Method B is uncurtailed and very time-consuming.

The following expedients are intended to drastically reduce computer running time. The objective functions do not represent the maximum value of power distribution as a solution of the neutron balance equation. No distinction is made between the rapid and the normal modes, and the Haling calculation is performed by the normal mode as in Methods A and B described above each time before the exploratory search mode is started for preparing the EOC k_∞ distribution and the base power distribution $P_{\text{form}ij}$ (Methods D and E).

Method C The power distribution P_{ij} is calculated with

$$P_{ij}=0.25k_{\infty ij}\Big(\sum_{l=1}^{4} k_{\infty ij}^{l}+\alpha_{ij}k_{\infty ij}\Big)\bar{k}_\infty/k_{\infty k}^{*} \quad (1)$$

as the initial base point, where $k_{\infty ij}^{l}$ $(l=1\sim4)$ represents the value of k_∞ of the four assemblies nearest to the location (i, j) and α_{ij} represents the value of albedo. The core average of k_∞ $(\bar{k}_\infty)$ and the corresponding region average $k_{\infty k}^{*}$, used for calculating the multiplier $\bar{k}_\infty/k_{\infty k}^{*}$ are taken from the Haling calculation of the initial base point. The value of P_{ij} without this multiplier represents the relative worth of a small region around the location (i, j). The multiplier is a normalization factor.

To minimize Eq. (1) is equivalent to reallocating $k_{\infty ij}$ such that an assembly of large k_∞ is placed next to an assembly of small k_∞ in a two-dimensional grid.

Method D The power distribution P_{ij} is calculated with

$$P_{ij}=0.25k_{\infty ij}\Big(\sum_{l=1}^{4} k_{\infty ij}^{l}+\alpha_{ij}k_{\infty ij}\Big)P_{\text{form}ij} \quad (2)$$

as the initial base point. Without the multiplier $P_{\text{form}ij}$, P_{ij} is the same as in Eq. (1). This multiplier $P_{\text{form}ij}$ is an empirical weighting factor.

Method E The power distribution P_{ij} is calculated with

$$P_{ij}=\sqrt{0.25k_{\infty ij}\Big(\sum_{l=1}^{4} k_{\infty ij}^{l}+\alpha_{ij}k_{\infty ij}\Big)P_{\text{form}ij}^{2}} \quad (3)$$

as the initial base point. Without the multiplier $P_{\text{form}ij}^{2}$, P_{ij} represents the effective k_∞ of a small region around the location (i, j), and the multiplier $P_{\text{form}ij}^{2}$ represents the importance of the location (i, j). Thus, to minimize Eq. (3) is equivalent to making the reactivity distribution as uniform as possible.

Method F The power distribution P_{ij} is calculated with

$$P_{ij}=0.25\Big|(k_{\infty ij}-k_{\infty k}^{*})\Big\{\sum_{l=1}^{4}(k_{\infty ij}^{l}-k_{\infty k}^{*l}) \\ +\alpha_{ij}(k_{\infty ij}-k_{\infty k}^{*})\Big\}\Big|\times 1{,}000 \quad (4)$$

as the initial base point. To minimize Eq. (4) means to reallocate $k_{\infty ij}$ such that an assembly of k_∞ greater than the region-wise average value is placed next to an assembly of k_∞ smaller than the same region-wise average value.

4. Immobilized Fuel Constraint

Skipping the locations of stuck fuel assemblies, if any, the assemblies in each region are numbered sequentially from maximum power density toward minimum. This preliminary treatment provides for the exploratory search to automatically prevent the stuck fuel assemblies from being shuffled.

5. Stuck Rod Margin Constraint

For each exchange in the exploratory, standard and exhaustive searches, the stuck rod margin is checked for all the control rods at several exposure points. In order to save computing time, the power distribution is fixed—irrespective of burnup—at that of the initial base point calculated immediately preceding initiation of each exploratory search, and controlled and uncontrolled k_∞ of each fuel assembly at these exposure points are calculated beforehand on the basis of this power distribution prior to commencement of each exploratory search mode. It is to be noted that this calculation of k_∞ is based on cold condition.

If an exchange results in violation of the stuck rod margin constraint, i.e. if A_{km}—the maximum value taken by the eigenvalue with one rod stuck in the range covering all the control rods at all the exposure points—exceeds a specified input value A_{kmax}, then the objective function is switched to $10A_{km}$ from the power peaking. If such violation does not take place, then the function is set at the maximum value of P_{ij} defined in Sec. 3 above.

The direct search procedure aims at finding an exchange that would minimize A_{km}, the stuck rod k_{eff}, until this constraint comes to be satisfied if it is not so at the initial base point, and if it is satisfied at this point, the procedure seeks an exchange that minimizes the radial power peaking f without violating the constraint. This is possible because $10A_{km}$ is always greater than f.

III. NUCLEAR REACTOR MODEL

The radial power distribution (Haling or normal) is calculated by a one-group, two-dimensional coarse mesh BWR simulator with use made of a nuclear thermal hydraulic coupled model. Comparison with three-dimensional calculations by FLARE[19] indicated that the results of the two-dimensional calculations gave reasonable agreement (eigenvalue within an error of 0.2%, cycle length within 3% and assembly power within 3%), provided that good estimates of the standard axial power and exposure distributions were available.

Fuel and bundle types are identified for dealing with axially distributed Gd_2O_3 burnable poison. The three-dimensional infinite multiplication factor $k_{\infty ijk}$ and moderator density U_{ijk} are calculated using the input axial power distribution P_k and the calculated assembly power distribution P_{ij} at each void loop iteration. The axial exposure distribution can serve as input for each assembly. If the input is not given for each assembly, a standard axial exposure distribution can be used for all assemblies. Source calculations are performed in two-dimensional geometry using the effective $k_{\infty ij}$, which is a P_k^2-weighted average of $k_{\infty ijk}$ over the axial range.

Consideration must indispensably be given to the effect on k_∞ brought by axial non-uniformity of void and exposure distributions, even for a two-dimensional BWR analysis. Experience indicates that P_k is well represented by a radially averaged axial distribution of the three-dimensional Haling power, which does not depend very sensitively on the detailed fuel loading pattern, and is determined in large part by the cycle number. This is also true for cold state analyses, in which the cyclewise axial power distribution at cold state similarly requires to be provided.

IV. SIMPLE EXPRESSION FOR STUCK ROD MARGIN

The direct search described in Chap. II normally requires at least 2,000 power distribution calculations. The number of control rods to be checked is 30 to 50 even for the quarter-core analysis of a symmetrical fuel loading pattern. This means that the number required of stuck rod margin calculations amounts to at least as much as 180,000 assuming three points to be checked for one

cycle.

Fortunately, single rod sticking is a strongly localized phenomenon, and hence it can be expected that the worth of the stuck rod can well be estimated by the characteristics of surrounding assemblies. **Figure 2** is the control rod configuration of a 460 MWe BWR in quarter-core representation. For convenience, the control rods are numbered from 1 to 30 in circular sequence from the core center toward the periphery. Two different reloading patterns for the second cycle were chosen for the analysis of stuck rod margin using a three-dimensional BWR simulator. The fuel
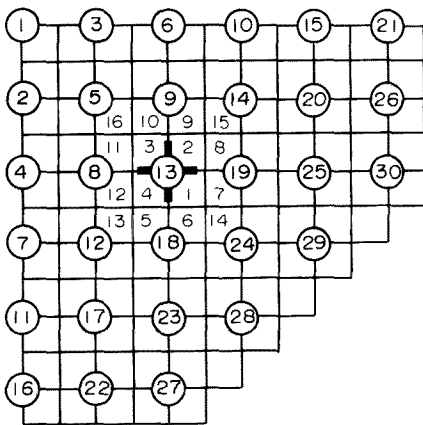
Fig. 2 Control rod configuration of typical BWR, with 16 assemblies around control rod
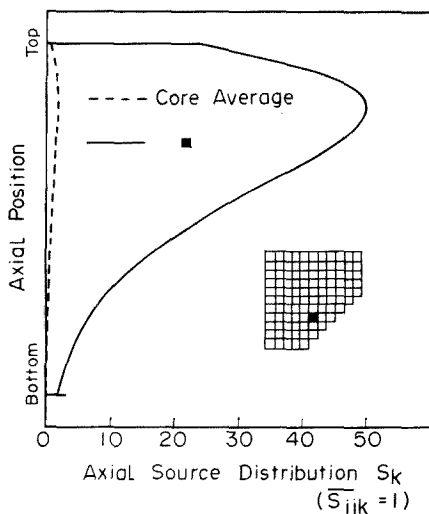
Fig. 3 Axial source distribution with control rod No. 28 stuck

assemblies were loaded in four-leaf symmetry, and full core analyses were performed to calculate the stuck rod margin for a rod sticking in each of the 30 control rod positions, with the rest fully inserted. **Figure 3** shows the axial neutron source distribution of the location marked ■ when the control rod No. 28 is stuck. In comparison with the core averaged distribution (dotted curve), the amplitude of the source distribution around the stuck rod is strikingly high, and evidences the strongly localized character of the phenomenon of rod sticking.

For qualitative analysis, the eigenvalue relevant to each position of rod sticking is plotted in **Fig. 4** for the average infinite multiplication factor $\bar{k}_\infty^U$ of the surrounding four assemblies in uncontrolled cold state. The infinite multiplication factor of an assembly (i, j) is defined here by

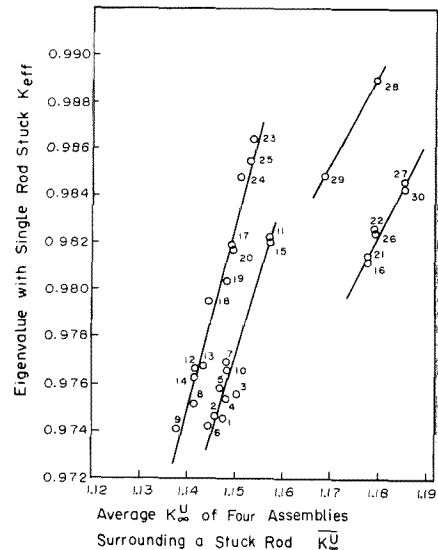$$k_{\infty ij} = \sum_k S_{ijk}^2 \cdot k_{\infty ijk} / \sum_k S_{ijk}^2 . \qquad (5)$$

Fig. 4 Relation between eigenvalue and average infinite multiplication factor of four assemblies surrounding a stuck rod

Examination of Fig. 4 reveals that the plots fall into four main groups, each distinguished by a straight line on which the plots are found:

Group 1: 16, 21, 22, 26, 27, 30
     2: 28, 29
     3: 8, 9, 12, 13, 14, 17, 18, 19, 20, 23, 24, 25
     4: 1, 2, 3, 4, 5, 6, 7, 10, 11, 15.

All the control rods in groups 1 and 2 are located near the core periphery, while those in group 3 are characterized by their being located adjacent to a fresh fuel assembly. Bearing in mind this particularity, the plots in groups 3 and 4 are treated as one group for both reloading patterns, and fitted by least squares method using the controlled and uncontrolled k_∞ of 16 surrounding assemblies. The numbers of the 16 assemblies around a stuck control rod is also shown in Fig. 2 for the rod 13.

The eigenvalue with one rod n stuck is expressed by

$$k_{\text{eff}}^n = \left\{ a_0 + a_1 \sum_{i=1}^{4} F_{ax_i} k_{\infty i}^u / 4 + a_2 \sum_{i=5}^{12} k_{\infty i}^c / 8 \right.$$
$$\left. + a_3 \sum_{i=13}^{16} k_{\infty i}^c / 4 \right\} R_{dfc_n}, \qquad (6)$$

where F_{ax_i}: Correction factor applied to fresh fuel assemblies with zero exposure
$a_0 \sim a_3$: Constants
R_{dfc_n}: Edge correction factor

and the suffixes u and c respectively denote uncontrolled and controlled states.

The rods in groups 1 and 2 are evaluated through multiplication by an edge correction factor. Not all the 16 assemblies are represented for the control rods 16, 22, 27, 28, 29, 30, 26, 21. For these cases, the effective $k_\infty^{u \text{ or } c}$ is generated for the missing assemblies by multiplying the k_∞ of the nearest edge assemblies by their albedo. It should also be noted that the assemblies Nos. 5~12 inclusive are not all controlled (e.g. assembly No. 8 of rod No. 27). For the reference 460 MWe BWR, these values prove upon calculation to be:

$a_0 = 0.21061$, $a_1 = 0.48176$, $a_2 = 0.19060$,
$a_3 = 0.02669$
$F_{ax_i} = 1.0$ for an assembly already in service
$= 1.025$ for a fresh assembly
$R_{dfc_n} = 1.0195$ for control rods 28, 29
$= 1.0247$ 〃 16, 21, 22, 26
$= 1.0361$ 〃 27, 30
$= 1.0$ for others

Figure 5 represents a comparison of the estimated values by fitting Eq. (6) with the original values obtained by three-dimensional

analysis. The standard deviation of this fitting is 0.09% and the maximum error 0.27%.

Other check calculations were performed to evaluate the accuracy of the three-dimensional calculation itself. Experimental data were taken from the first cycle startup experiment of a 460 MWe BWR for comparison with calculations on the cold critical control rod configuration. The eigenvalues of the three-dimensional calculations were found to be 1.0031 for the A rod pattern and 0.9997 for the B rod pattern. These results can be considered satisfactory, at least for first-cycle analyses.
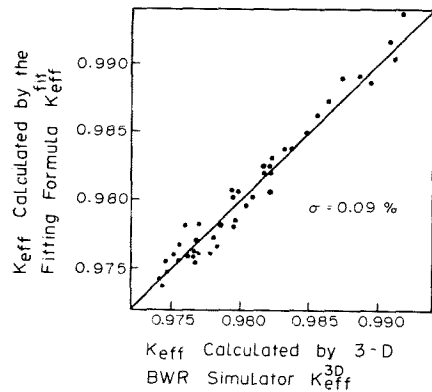

Fig. 5 Accuracy of fitting formula for stuck rod margin

V. RESULTS AND DISCUSSION

The method described in the previous chapters was applied to fuel loading pattern optimization for the second and equilibrium cycles of a 460 MWe commercial BWR. Two different loading principles were tried separately for both cycles with and without the stuck rod margin constraint. The first principle applies no constraint on the positions for fresh fuel placement (1st example), while the second prescribes their locations in a regular arrangement (2nd example). For each case, the fuel loading pattern is four-leaf symmetrical.

First, the effects of differences in the objective functions (Methods A~F) and in the initial guess on the convergence speed and on the optimized pattern were examined for the second cycle loading without the stuck rod margin constraint. Next, the effect of the

stuck rod margin constraint was added for both the second and equilibrium cycle loadings.

Figure 6 shows the burnup spectra at the end of the first and equilibrium cycles. That after the first cycle was obtained by estimating the state of the initially loaded reactor with poison curtain arranged on Haling principle as it would be upon complete burnup to the point of no residual reactivity. The length of the cycle is 1.37 yr with a load factor of 80%. The second cycle starts after removal of all the poison curtains and upon proper refueling. All cycles thereafter are set to last 1.0 yr with the load factor unchanged. The number of fresh fuel assemblies can range from 8 to 14 (quarter core) depending on the choice of the EOC target k_∞ distribution. In the present instance, 13 was chosen for the first example and 14 for the second. It should be noted that whether with or without stuck-rod constraint, the core is very reactive in cold state, which makes it difficult to satisfy the stuck rod margin constraint.
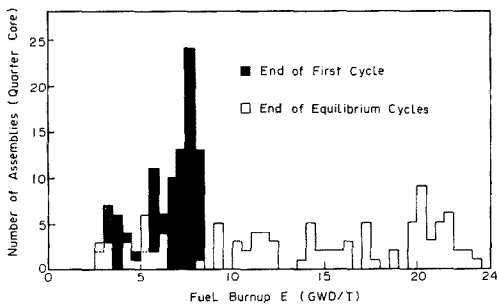

Fig. 6 Burnup spectra of first and equilibrium cycles

The spectrum representing the end of equilibrium cycle was taken from that obtained after running OPREF for 20 cycles. The number of fresh fuel assemblies ranges from 18 to 23, again depending on the choice of EOC target k_∞ distribution; here, 21 was chosen for both examples. Compared with the second cycle, the number of reload fuel assemblies is much larger for the equilibrium cycle, where about 1/5 of the core is replaced. This is due to the reactivity gain obtained by the removal of the poison curtain and to the relatively low exposure of the remaining as-

semblies in the second cycle.

For both the second and the equilibrium cycle refuelings, the EOC target k_∞ distribution was so chosen that the global power peaking became about 1.2. The assemblies discharged were those with the largest burnup, and the region-wise shuffling scheme was based on the OPREF results.

1. Effect of varying Objective Functions on Radial Power Peaking and Initial Guesses

The direct search algorithm does not yield the true optimum; only a local optimum is given, and it remains to evaluate the true validity of this optimum. To this end, an initial guess pattern was devised, which was intentionally distorted by lumping together all the fresh fuel assemblies into a small region. This guess pattern is shown in the upper left-hand side of **Fig. 7**. The numbers marked in the diagrams indicate the 10 assemblies contributing the largest power. These assemblies, seen lumped together, are all fresh fuel. The corresponding assembly power distribution is shown in the upper right for the three radial directions A-A', B-B' and C-C'. The radial power peaking is 1.485, which is quite prominent. This initial guess pattern was adopted as starting point for comparing Methods A~F with the exception of B.

The pattern optimized by Method A is reproduced on the lower left-hand side of Fig. 7, with the corresponding assembly power density distribution shown at right (We shall
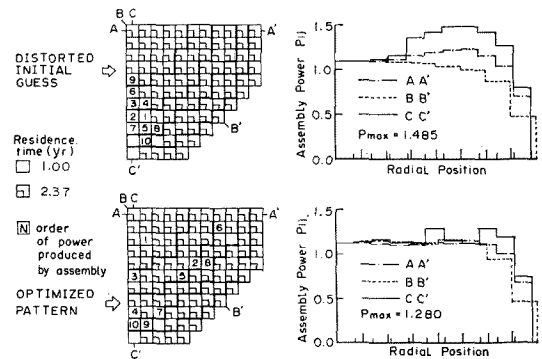

Fig. 7 Power distributions (right) of initial guess and optimized patterns (left)—Case S1BAN

designate this case S1BAN=Second cycle, 1st example, Bad guess, method **A**, No stuck rod margin constraint). This solution is seen to have brought down the radial power peaking from 1.485 to 1.280. The point of maximum power is located at the position of fresh fuel assembly in the first region, all the remaining high-power assemblies marked by numbers in the diagram are also fresh fuels. The optimized power distribution is multi-modal, and the assemblies occupying the highest several rankings are seen to register power densities very close to each other. Geometrically, the fresh fuel assemblies are better scattered than with the initial guess pattern, but are still somewhat agglomerated.

In so far as concerns the power distribution, these localized groups of fresh fuel assemblies do not cause power peaking thanks to their being placed outside the central region of the core, and their reactivity is suppressed by Gd_2O_3 burnable poison. Actually, the reactivities of the freshly loaded fuels at BOC (beginning of cycle) are much smaller than those of the partly burned initial fuels carried over to the second cycle. At EOC, however, the newer fuels exceed the older in reactivity, and come to give higher power densities on the average, by Haling power distribution.

The stuck rod margin for the optimized pattern is 0.17% (Δk) and the strongest rod is No. 28 at BOC. The solution does not satisfy the stuck rod margin constraint, which was expected. A_{kmax} is set at 0.99 for this constraint in the present instance.

Figure 8 shows how the radial power peaking is reduced in the process of direct search optimization. The number of trial exchanges is 110, of which 14 pairs of exchanges are successful. Four tables were generated and four Haling power distributions calculated by the normal mode, while 14 normal power distribution calculations were performed for the normal mode and 2207 for the rapid mode. The computer time required was about 300 sec by IBM 370/158. The average time for calculating one power distribution was 0.15 sec.

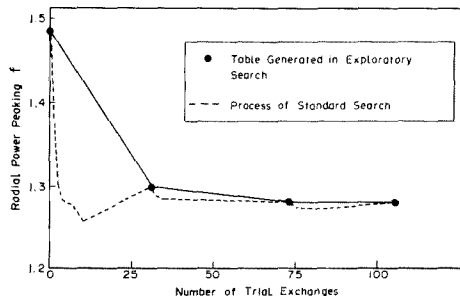It is noted that the power peaking always diminishes in the standard search mode, but

Fig. 8 Process of optimization by direct search—Case S1BAN

normally increases in the recalculation of the ensuing initial base point. This is because in Method A a simple normal power distribution is substituted for the Haling distribution. What counts is the efficacy of the search procedure and the validity of the final result. The final power peaking of 1.280 obtained in the present case is considered acceptable. The standard search algorithm has an advantage over the case where the exhaustive mode has to be adopted from the outset.

Examination of the exchanged assemblies give rise to some interesting observations: None of the 14 exchanged pairs of assemblies represent an assembly of maximum power. The rankings of regions in terms of the maximum power density and the regions in which the exchanges were made are shown in **Table 1**. It is seen that in the 1st exploratory search, the assemblies exchanged are in the regions of high power densities, whereas they are found mainly in the low power regions in the 3rd search. This means that the low power assemblies play an important role in further reducing the power peaking of a reasonably

Table 1 Rankings of regions in terms of maximum power density and regions of exchanged assemblies for Case S1BAN

Exploratory search	Region rankings				
	1st	2nd	3rd	4th	5th
1st	③	②	①	4	5
2nd	2	③	①	4	5
3rd	①	2	3	④	⑤
4th	1	2	3	4	5

Note: Region numbers enclosed in circles indicate that assemblies are successfully exchanged in these regions.

flattened loading pattern.

The principal factor that controls the power distribution is k_∞, and it remains to find a general rule governing the local arrangement of the k_∞ distribution. For an infinitely large continuously refueled reactor, Kawai & Kiguchi[20] have derived the rules of farthest distance and of maximum exposure of neighboring fuels. Methods C~F are based on these rules applied to a batch refueled BWR. **Figure 9** shows how the peaking index (maximum value of Eq. (3)) is reduced by direct search with Method E, which we shall call case S1BEN (Second cycle, 1st example, Bad guess, method **E**, **N**o stuck rod margin constraint).
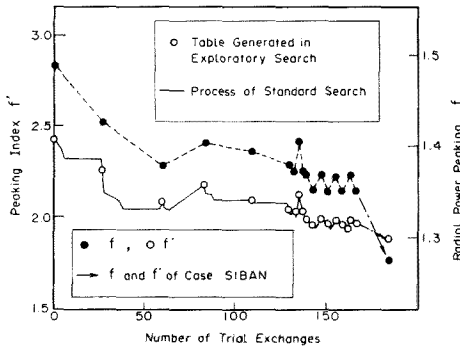

Fig. 9 Process of optimization by direct search—Case S1BEN

The corresponding radial power peaking is indicated by the right-hand scale. The peaking index has a strong correlation to power peaking, which means that reducing the peaking index is equivalent to reducing the power peaking. It is seen, that the direct search does not converge towards optimum, but ends in oscillatory behavior. The other methods have also shown similar behavior. The local nature of Eqs. (1) to (4) would appear to be the cause of this.

To verify the validity of the objective functions, the peaking indexes of the results obtained with Methods C~F were calculated for the optimized pattern of case S1BAN. An example for Method E is indicated by the arrow mark in Fig. 9, which evidences the effective reduction of peaking index. Method D revealed a similar effect, but not Methods C and F, which yielded the values larger than that at the outset of oscillation. Physical con-

siderations would indicate that when the pattern is already flattened to some extent, the effect of spatial neutron importance surpasses that obtained by local k_∞ arrangement, and that is why Methods D and E, which include the spatial weight $P_{form_{ij}}$ and $P_{form_{ij}}^2$, show better results than others. This surmise is substantiated by a comparison of the locations of maximum peaking index: With Eqs. (2) and (3) the maximum is located at the position of the second ranking in power density obtained on the optimized pattern with Method A, whereas with Eqs. (1) and (4) the corresponding position is that of the tenth in ranking.

While none of Methods C~F converged towards optimum, Methods D and E, and particularly E appear the most promising. These method require less than 1/10 of the time required for generating one table compared with Method A, which would make it quite feasible to combine these methods with some other technique such as random search. Methods D and E show possibility of rapidly yielding the optimal pattern through power distribution calculations repeated several times combined with many calculations of the local factor.

We next compare Method B with Method A applied to a reasonably good guess. Such a guess is obtained by the MIKDM (minimum integrated K-deviation method[16]), as shown in the upper left-hand drawing of **Fig. 10**, with the corresponding power distribution shown at right. The power peaking is 1.311.
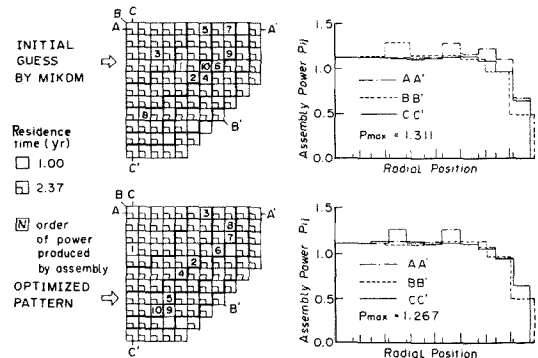

Fig. 10 Power distributions (right) of initial guess and optimized patterns (left)—Case S1GBN

The result of optimization by Method B and the corresponding power distribution is shown in the lower half of the same Fig. 10 (Case S1GBN [Second cycle, 1st example, Good guess, method **B**, No stuck rod margin constraint]). The power peaking is 1.267. Before proceeding to a comparison with Method A, it might be remarked that case S1GBN represents a 1% reduction in power peaking in reference to case S1BAN, which can be hardly considered a significant difference. The stuck rod margins is 0.33%. The strongest rod is No. 29 at BOC.

Methods A (S1GAN) and B (S1GBN) are mutually compared in **Fig. 11**, which retraces the process of optimization. The final result obtained with Method A is a minimized power peaking of 1.268, which again is essentially the same as obtained by Method B. But the optimized patterns are not very similar to each other. It is worth noting that Method B reduces the power peaking consistently throughout the search process, but that it requires a computing time of about 7,800 sec, which is more than 15 times that for Method A (about 500 sec). Comparison between cases S1GAN and S1GBN also clearly evidences the better efficiency provided by Method A.
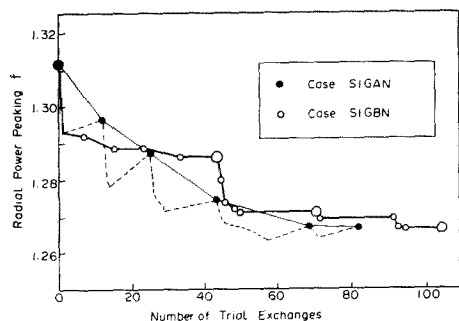

Fig. 11 Process of optimization by direct search—Case S1GAN and case S1GBN

On the other hand, comparison of case S1GAN with case S1BAN reveals the effect of the difference in initial guess patterns. A further trial was performed to obtain a measure of the ease of optimization procedure. The two-dimensional BWR simulator described in Chap. III was reprogrammed for TSO (time sharing option) application. Starting from the

same MIKDM guess, improvement of the loading pattern was sought by man-machine conversational system using a graphic-display computer facility (IBM 3270). It was found very difficult to further reduce the power peaking from 1.311. The best result obtained after a session of more than 4 hr was 1.299 which does not even equal the result obtained with case S1BAN. The MIKDM guess is already well flattened, to the extent that mere exchange of the highest power assembly with one of lower power can no longer contribute significantly to further pattern improvement. This side experiment may be considered to attest conclusively to the efficacy of the direct search method presented here for the most guess patterns encountered in actual practice, and that efforts spent for further refinements should have little practical value.

2. Effect of Stuck Rod Margin Constraint

The final aim of this paper is to show that the direct search algorithm can take into account the stuck rod margin constraint, and also to show how the optimized solution is affected by this constraint. In the following analysis, the stuck rod margin constraint is checked at three points in the burnup cycle: BOC, HOC (half of cycle) and EOC, adopting a limiting stuck rod margin of 1% Δk (A_{kmax} =0.99).

Figure 12 shows the optimized pattern (left) and the power distribution (right) for the case S1BAS (Second cycle, 1st example, Bad guess, method **A**, Stuck rod margin constraint). The results should be compared with case S1BAN of Fig. 7. The radial power peaking is 1.289, which is 0.7% higher than without the constraint. Superficial comparison between the resulting optimized patterns obtained for case S1BAS and case S1BAN (*i.e.* with and without constraint) reveals no appreciable difference between the two cases. The intrinsic difference lies in the searching process, reproduced in **Fig. 13**. The stuck rod margin of the first initial base point is $-0.1\% \Delta k$, which means that a single rod stuck can leave the reactor critical. The strongest rod is No. 11 at EOC. The locally arranged reload fuel
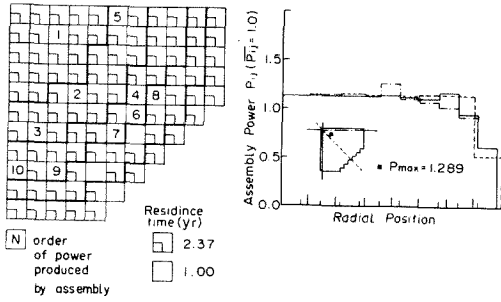
Fig. 12 Optimized pattern (left) and power distribution (right)—Case S1BAS

becomes highly reactive at EOC on account of the depletion of the Gd_2O_3 burnable poison. Since the constraint is not satisfied, the direct search tries to minimize k_{eff} with the single rod stuck (*i.e.* maximize the stuck rod margin Δk^s). From the second initial base point onwards, the strongest rod moves toward the periphery (rod Nos. 27~29). The search resulted in a feasible solution at the 10th standard search, whence the objective function was switched to focus on radial power peaking— to find the optimum pattern among those that satisfy the constraint. The stuck rod margin of the finally optimized pattern is 1.0%, precisely at the imposed limit of the constraint. The strongest rod is No. 29 at BOC.
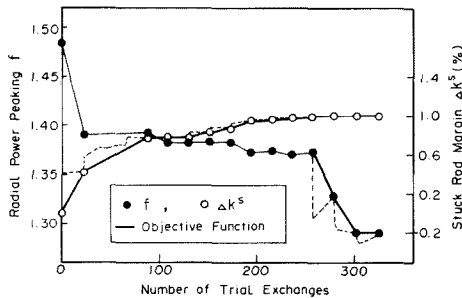

Fig. 13 Process of optimization by direct search—Case S1BAS

The resulting pattern has the fresh fuel assemblies still somewhat agglomerated, but not to the extent of excessively raising the power peaking or reducing the stuck rod margin. The limiting factor is represented by the partially burned-up initial fuel assemblies placed near the core periphery. They are less burned-up than those in the core center and hence more reactive. The EOC

target k_∞ is largest in the outermost region. This is necessitated by the requirement to minimize the excess reactivity induced by the withdrawal of all the poison curtains and the insertion of as many as 13 fresh fuel assemblies.

As stated earlier, the core is very reactive in cold state for the second cycle, imposing strong limitations to satisfaction of the stuck rod margin constraint. Nevertheless, Figs. 12 and 13 reveal that the direct search method can accommodate the stuck rod margin constraint even for this very severe situation, with little sacrifice of power peaking. The time required for computing case S1BAS is about 1,500 sec, which is considerably longer than for case S1BAN. The poorer efficacy of the search process is partly due to the geometrical locality of Eq. (6) which slows down the rate of convergence toward satisfaction of the constraint. The additional time required to calculate Eq. (6) is about 30% for Method A. But the computing time of 1,500 sec is thought to be still acceptable.

Figures 14 and **15** show another example of the second cycle, case S2GAS (Second cycle, 2nd example, Good guess, method **A**, Stuck rod margin constraint), in which the locations of the fresh fuel assemblies are fixed. The im-
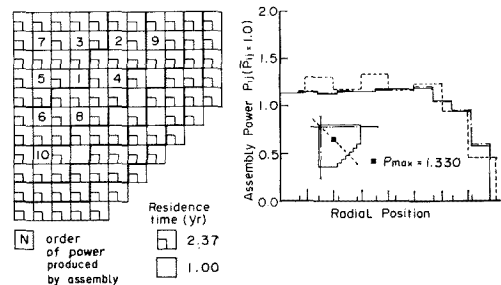

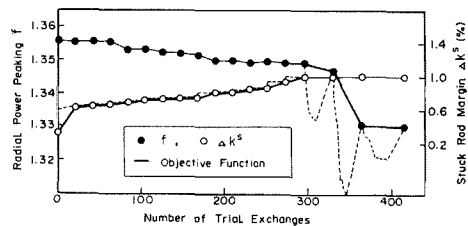**Fig. 14** Optimized pattern (left) and power distribution (right)—Case S2GAS

Fig. 15 Process of optimization by direct search—Case S2GAS

mobilized fuel option is used for this purpose. This type of fuel loading is often adopted in actual practice. The power peaking of the optimized pattern is 1.330 and the stuck rod margin 1.01%, the former being considerably higher than in the case of case S1BAS, while the stuck rod margin is much the same. **Table 2** shows the stuck rod margin distribution. The strongest rod is No. 28 at BOC. Here again the fresh fuel is not that which causes the highest rod worth.

Table 2 Stuck rod margin Δk^s (%) for optimized pattern—Case S2GAS

3.19	3.59	3.70	2.74	1.26	2.50
3.59	3.37	3.30	2.50	1.86	3.50
3.70	3.36	3.14	2.16	1.12	1.95
2.74	3.07	2.88	1.93	1.05	
1.26	1.73	1.34	1.01		
2.50	2.86	2.54		$t = 0.0$ yr	

5.30	5.45	5.56	4.66	3.12	3.98
5.45	4.61	4.55	3.77	3.21	4.94
5.56	4.60	4.39	3.41	2.36	3.16
4.66	4.30	4.12	3.20	2.01	
3.12	3.03	2.59	2.54		
3.98	4.29	3.67		$t = 0.5$ yr	

7.43	7.43	7.56	6.71	5.15	5.55
7.43	6.08	6.06	5.30	4.65	6.41
7.56	6.08	5.89	4.87	3.62	4.48
6.71	5.74	5.49	4.45	2.71	
5.15	4.42	3.77	4.04		
5.55	5.77	4.83		$t = 1.0$ yr	

In order to evaluate the accuracy of the method, the power peaking, the cycle length and the stuck rod margin have been recalculated by a three-dimensional BWR simulator for case S2GAS. The results are summarized in **Table 3**. The stuck rod margin calculated

Table 3 Comparison of result obtained for Case S2GAS with that of three-dimensional analysis

	OPREF	3-D simulator	Error (%)
Exposure (GWD/T)	4.745	4.895	−3.1
Radial power peaking	1.330 (4, 8)	1.297 (4, 8)	2.5
Stuck rod margin	1.01 (rod No. 28)	0.96 (rod No. 23)	5.2

by the simulator showed a roughly 5% smaller value, and also the strongest rod was not the same. A more precise treatment of axial weighting and of the peripheral rods would appear necessary for improving the accuracy of OPREF.

The foregoing comparison between cases S1BAS and S2GAS, would not appear conclusively in favor of the latter over the former, at least within the scope of the present results. A possible objection against case S1BAS might be the marked non-uniformity of the power density changes with time, which may give rise to some difficulty in generating the long-term control rod withdrawal sequence.

Thus far the discussion has been limited to the second cycle refueling. The same treatment can be applied to the equilibrium cycle refueling.

Figures 16 and **17** show the results of case E1GAS (Equilibrium cycle, 1st example, Good guess, method A, Stuck rod margin constraint). All of the assemblies are recharge fuel loaded with Gd_2O_3 burnable poison. The assemblies fall into five different groups according to the time of their loading into the core. Power mismatching between these assemblies is much larger than that in the second cycle, which occasions a slightly larger power peaking in the optimized pattern. Some of the fresh fuel assemblies are placed next to each other, but still do not produce high power peaking. The assemblies of different groups are not uniformly distributed. Optimal region wise shuffling by OPREF precludes uniform scatter loading on account of the non-uniform optimal EOC k_∞ distribution[16]. Region-wise shuffling mainly modifies the global power shaping,

Fig. 16 Optimized pattern (left) and power distribution (right)—Case E1GAS

Fig. 17 Process of optimization by
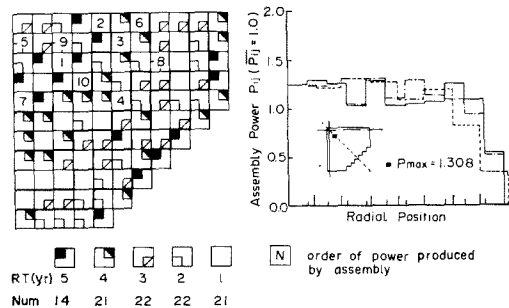direct search—Case E1GAS

Fig. 18 Optimized pattern (left) and power
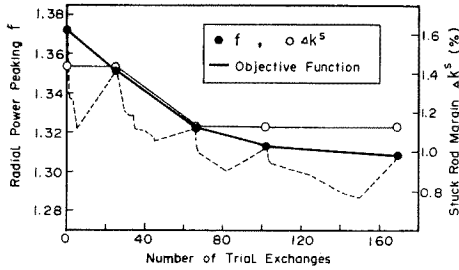distribution (right)—Case S2GAS

Fig. 19 Process of optimization by
direct search—Case E2GAS

while the in-region allocation treated here con-
tributes to the reduction of assembly mis-
matching.

The core at cold state is less reactive than
in the second cycle due to the large spread
of the burnup spectrum, which is why the
initial guess pattern by MIKDM satisfied the
stuck rod margin constraint, and this is what
rendered the search process in Fig. 17 essen-
tially the same whether with or without the
constraint. The stuck rod margin of the
optimized pattern is 1.13%. The strongest
rods are Nos. 2 and 3 at BOC (they have the
same value on account of the four-leaf symmetry).
In contrast to the second cycle, no problem
is posed by the peripheral rods, nor, in general
in satisfying the stuck rod margin constraint.
The computing time is about 400 sec.

Figures 18 and **19** show the results obtained
for case E2GAS (Equilibrium cycle, 2nd exam-
ple, Good guess, method A, Stuck rod margin
constraint), in which the fresh fuel assemblies
are fixed at certain location. This fixation of
charging location strongly reduces the degree
of freedom for reallocation, which results in
an optimized pattern of 1.385 power peaking
—considerably higher than in the previous
cases. The region wise shuffling scheme is
much the same as in case E1GAS, so that the
solution has no resemblance to uniform scatter
loading. Pure uniform scatter loading with
little regionwise shuffling requires the dis-
charge of less burned fuel assemblies, which
in turn results in a larger fuel inventory,
although the power peaking may be smaller.
What is more, the inverse of the fraction of
each fuel group is no longer always an integer.
This complicates the geometrical arrangement
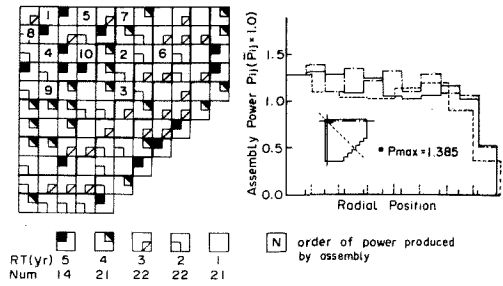of pure scatter loading.

Table 4 presents the stuck rod margin of
each control rod. Its distribution is spatially
irregular, depending to large extent on the
local arrangement of the loading pattern. The
strongest rod is No. 23 at BOC and the margin
1.53%.

Table 4 Stuck rod margin Δk^s (%) for
optimized pattern—Case E2GAS

1.97	3.36	3.67	5.49	3.02	5.77
3.36	5.57	5.26	2.55	2.22	7.00
3.67	5.37	5.59	1.67	2.06	5.68
5.49	6.01	1.69	2.98	4.82	
3.02	4.78	1.53	4.10		
5.77	3.74	3.61		t = 0.0 yr	

3.53	4.34	4.67	6.51	3.52	6.00
4.34	6.58	6.28	3.59	2.52	7.60
4.67	6.30	6.61	2.05	2.61	6.37
6.51	7.02	2.60	3.82	5.82	
3.52	5.68	1.64	4.24		
6.00	4.57	4.18		t = 0.5 yr	

5.57	5.90	6.12	7.82	4.66	6.57
5.90	8.01	7.65	5.07	3.75	8.05
6.12	7.63	7.95	3.48	3.61	6.73
7.82	8.22	3.95	4.97	6.90	
4.66	6.66	2.55	4.73		
6.57	6.70	6.08		t = 1.0 yr	

All the cases treated in this study bring the lowest point of the stuck rod margin to the BOC notwithstanding the provision of fuel loaded with Gd$_2$O$_3$ burnable poison.

Verification of this constraint can be performed only at BOC.

VI. CONCLUSION

The direct search algorithm originally proposed by Naft & Sesonske was applied to optimization of the fuel assembly allocation for a BWR. Extensive consideration was given to the determination of a suitable nuclear reactor core model and the treatment of operating constraints. The procedure can be followed quite mechanically. A characteristic feature is the explicit inclusion of the stuck rod margin constraint in the optimization process.

Full application of the direct search procedure requires power distribution calculations at EOC to be repeated several thousand times and for each resulting eligible fuel loading pattern, the stuck rod margin constraint has to be checked separately for each control rod at several points in the burnup cycle. To simplify this procedure, a simple expression was developed for evaluating the stuck rod margin, based on least squares fitting of the nuclear data around a stuck rod to the results of three-dimensional full core analysis at cold state with 0.09% as standard deviation. In an effort to further reduce the computer running time, a comparison was made of several alternative procedure for calculating the objective function to evaluate the radial power peaking in terms of values based on the Haling power distribution. Of six such alternative procedures, the first one indicated satisfactory convergency within a reasonable computing time (500 to 1,500 sec by IBM 370/158), in which the exact Haling power distribution is calculated only once prior to each exploratory search, and on other occasions the normal power distribution with k_∞ of the initial base point exchanged is calculated, by either the normal or the rapid mode, depending on the situation.

The practical applicability of the method was confirmed through trial computations for the second and equilibrium cycles of a medium-sized commercial BWR of 460 MWe. The optimized pattern was found to satisfy the stuck rod margin constraint with minimum radial power peaking.

——REFERENCES——

(1) TABAK, D.: Optimization of nuclear reactor fuel recycle via linear and quadratic programming, *IEEE Trans. Nucl. Sci.*, NS-15, 60 (1968).
(2) WALL, I., FENECH, H.: The application of dynamic programming to fuel management optimization, *Nucl. Sci. Eng.*, 22, 285 (1965).
(3) STOVER, R.L., SESONSKE, A.: Optimization of BWR fuel management using an accelerated exhaustive search algorithm, *J. Nucl. Energy*, 23, 673 (1969).
(4) HOSHINO, T.: In-core fuel management optimization by heuristic learning technique, *Nucl. Sci. Eng.*, 49, 59 (1972).
(5) NAFT, B.N., SESONSKE, A.: Pressurized water reactor optimal fuel management, *Nucl. Technol.*, 14, 123 (1972).
(6) STOUT, R.B., ROBINSON, A.H.: Determination of optimal fuel loading in PWR using dynamic programming, *ibid.*, 20, 86 (1973).
(7) CHITKARA, K., WEISMAN, J.: An equilibrium approach to optimal in-core fuel management for pressurized water reactors, *ibid.*, 24, 33 (1974).
(8) KUBOKAWA, T., KIYOSE, R.: Optimization of in-core fuel management by integer linear programming, *Proc. Conf. Computational Methods in Nucl. Eng.*, Ⅲ-135, (1975).
(9) MÈLICE, M.: Pressurized water reactor optimal core management and reactivity profiles, *Nucl. Sci. Eng.*, 37, 451 (1969).
(10) THOMSEN, K.L.: Self-management, an approach to optimum core management of thermal reactors by means of ideal burnup distribution, *Risö* 232, (1971).
(11) SAUAR, T.O.: Application of linear programming to in-core fuel management optimization in light water reactors, *Nucl. Sci. Eng.*, 46, 274

(1971).

(12) SUZUKI, A., KIYOSE, R.: Application of linear programming to refueling optimization for light water moderated reactor, *ibid.*, **46**, 112 (1971).

(13) FORKNER, S.L., SPECKER, S.R.: An algorithm for determining optimum fuel management decisions with generalized cycle requirements, *Proc. Conf. Math. Models and Comput. Tech. for Analysis of Nucl. System, CONF*-730414, Ann Arbor (1973).

(14) ROTHROCK, R.B., GARLID, K.L., OMBERG, R.P.: Applications of non-linear programming techniques in multistage fuel management optimization, *ibid.*

(15) HOSHINO, T., TAKAHASHI, M., FUJII, Y.: Optimization of in-core fuel management, cycle period and power scheduling of nuclear power plants by large scale non-linear programming, *Proc. Conf. Comput. Methods in Nucl. Eng.*, III-115, (1975).

(16) MOTODA, H., HERCZEG, J., SESONSKE, A.: Optimization of refueling schedule for light water reactors, *Nucl. Technol.*, **25**, 477 (1975).

(17) HALING, R.K.: Operating strategy for maintaining an optimum power distribution throughout life, *Proc. ANS Topical Meeting, Nucl. Performance of Power Reactor Cores, TID*-7672, (1964).

(18) KAWAI, T., MOTODA, H., KIGUCHI, T., OZAWA, M.: A method for generating a control rod program for boiling water reactors, *Nucl. Technol.*, **28**, 108 (1976).

(19) DELP, D.L., *et al.*: FLARE-A three dimensional boiling water reactor simulator, *GEAP*-4598, (1964).

(20) KAWAI, T., KIGUCHI, T.: Optimum refueling order for minimum local power peaking factor, *Nucl. Sci. Eng.*, **43**, 342 (1971).